Silicon (2022) 14:5913–5921
https://doi.org/10.1007/s12633-021-01372-1

ORIGINAL PAPER

Design and Development of Graphene FET Biosensor for the Detection of SARS-CoV-2

B. Vamsi Krsihna[1] · Shaik Ahmadsaidulu[2] · Surapaneni Sai Tarun Teja[2] · D. Jayanthi[3] · Alluri Navaneetha[4] · P. Rahul Reddy[5] · M. Durga Prakash[2]

Received: 19 August 2021 / Accepted: 1 September 2021 / Published online: 12 September 2021

Abstract

The most affected disease in recent years is Severe Acute Respiratory Syndrome Coronavirus 2 (SARS-COV-2) that is notable as COVID-19. It has been started as a disease in one place and arisen as a pandemic throughout the world. A serious health problem is developed in the lungs due to the effect of this coronavirus. Sometimes it may result in death as a consequence of extensive alveolar damage and progressive respiratory failure. Hence, early detection and appropriate diagnosis of corona virus in patient's body is very essential to save the lives of affected patients This work evolves a Silicon (Si) based label-free electrical device i.e. the reduced graphene oxide field-effect transistor (rGO FET) for SARS-CoV-2 detection. Firstly rGO FET functionalized with SARS-CoV-2 monoclonal antibodies (mAbs). Then the rGO FET characteristic response is observed to detect the antibody-antigen reaction of SARS-CoV-2 with different molar ranges. The developed GFET shows better performance towards the drain current and limit-of-detection (LoD) up to 2E-18 M. Therefore, we believe that an intense response was observed than the earlier developed devices and signifies impressive capability for subsequent implementation in point-of-care (PoC) diagnostic tests.

Keywords FET · SARS-CoV-2 · rGO · Biosensor · Limit of detection

1 Introduction

Emerging contagious diseases, such as severe acute respiratory syndrome (SARS), Flu, and Ebola infection illness, pose a major risk to human health. In December 2019, a series of patients were admitted to the hospital with symptoms of pneumonia and severe acute respiratory syndrome (SARS) in a place named Wuhan, China. The causes for this disease were unknown initially. From there on, 2019 novel Covid (2019-nCov) was perceived inside the patient's nasal liquid. Subsequently, it was named again as Severe Acute Respiratory Syndrome Coronavirus 2 (SARS-CoV-2) [1, 2]. World Health Organization (WHO) alluded to this infection as Corona Virus Disease (Covid-19). It declared that the virus causes this disease as a 2019 novel coronavirus (2019-nCoV). On March eleventh, 2020 WHO recognized this Covid-19 as pandemic as it is transmitting among the people of different countries with rapid speed [3]. The basic symptoms of this disease may include fever, loss of taste or smell, dry cough, and fatigue. The severe symptoms of this disease may contain chest pain or pressure, shortness of breath or difficulty in breathing, and loss of speech or movement. This novel coronavirus is transmitted by droplets and aerosols of human saliva. The severity of this pandemic can be observed by the statistics provided by WHO.

The total number of cases globally is approximately 18.5 crores and the total deaths are 40 Lakhs up to July 1st week. Due to this pandemic entire world faced different socio-economic problems. To avoid these difficulties, the patients need to be properly diagnosed and treated with utmost care. Even though there are some measures to prevent or control this coronavirus, like WHO-recommended medicines or

✉ M. Durga Prakash
mdprakash82@gmail.com

[1] Department of ECE, Koneru Lakshmaih Education Foundation, Guntur 522502, Andhra Pradesh, India

[2] Department of ECE, Velagapudi Ramakrishna Siddhartha Engineering College, 520007 Kanuru, Andhra Pradesh, India

[3] Department of ECE, Gokaraju Rangaraju Institute of Engineering & Technology, 500090 Hyderabad, Telangana, India

[4] Department of ECE, Mahatma Gandhi Institute of Technology, 500075 Hyderabad, Telangana, India

[5] Department of ECE, Geethanjali Institute of Science and Technology, 524137 Nellore, Andhra Pradesh, India

vaccines but the human life is still having a threat from the Covid-19 pandemic (https://covid19.who.int/table), [4, 5].

The early detection of this Coronavirus disease in the fluids extracted from patients is utmost prioritized for proper treatment of the patients as this disease may become severe within 5–10 days. In this scenario, laboratory diagnostics is the major parameter to detect the disease even at lower concentrations. To fulfil the above needs, RT-PCR (polymerase chain reaction) is one of the nuclear-derived methods to detect the existence of a particular virus i.e., 2019-nCoV. This technique directly analyses the presence or absence of the virus's RNA.

Enzyme Linked Immunosorbent Assay (ELISA) analysis is another strategy to distinguish a particular antibody and antigen response. These diagnosis techniques take a longer period of 3 to 24 h for the results. Hence, there is a great need for bio-sensors that can detect the corona virus-like particles and a sensitive and quick method is required to identify the virus particles is required to treat this type of pandemic disease (https://www.iaea.org/newscenter/news/how-is-the-covid-19-virus-detected-using-real-time-rt-pcr), [6, 7]. In this study, we design GFET biosensor functionalized mAbs for rapid identification of COVID-19, as shown in Fig. 1.

The identification involves different steps like collection of samples from the patient, preserving it and finally compelling the sample to get responded with designed GFET. This work mainly aims to identify the presence of novel coronavirus particles through using a GFET and to report its characteristic changes in the presence and absence of coronavirus particles.

2 Design and Simulation of GFET

A GFET is designed and simulated with the semiconductor module of COMSOL Multiphysics. The dimensions of the designed sensor are gold contact length of 50nm, the thickness of graphene is 0.35nm is used for this design. The silicon dioxide layer with a thickness of 6nm acting as a dielectric layer with a dielectric constant of 4.2. The device parameters are shown in Table 1.

The semiconductor module in the software is used for analyzing the transfer characteristics and drain characteristics. The drain current is one of the vital parameters to analyze the enactment of the designed sensor. The drain current flows through the graphene layer only because, it acts as a channel for the conduction of drain current between drain and source and no other channel exists between drain and source. With this, the characteristics of the designed GFET were analyzed without any difficulty.

The electrical characteristics of the designed structure were calculated in the absence and presence of the coronavirus particles. These electrical characteristics are crucial parameters to determine the overall sensing performance of the device. Many important factors affect the electrical characteristics because the drain current varies with different parameters of the graphene channel [8]. The GFET designed with the software is shown in Fig. 2.

The software proficiently permits the assignment of different physical properties of the materials to the designed model as per the requirement. The fixed dimensions of GFET allow us to determine the presence and absence of coronavirus antigen protein (spike protein of SARS-CoV-2) along with immobilized monoclonal antibody. With the special characteristics of GFET sensors such as high sensitivity and biological molecule detection, they are making significant progress in the production of ultrasensitive bio-sensors for biochemical analysis. The identification of immobilized antibodies (mAbs) and antigens arise at the graphene channel of the GFET biosensor. The receptor molecule (antibody) is immobilized on

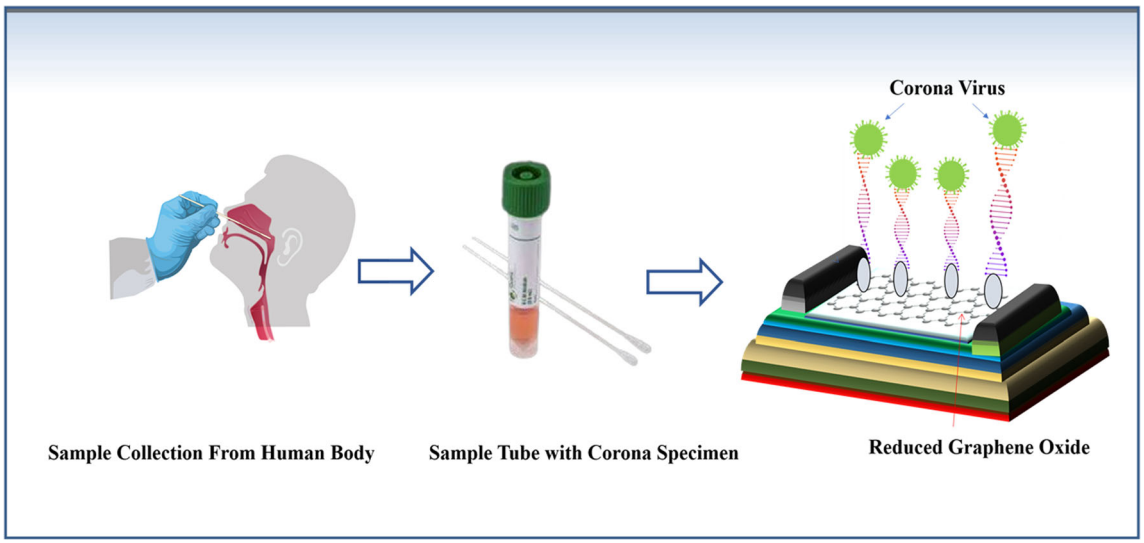

Fig. 1 Schematic diagram of SARS-CoV-2 detection using the rGO FET biosensor

Table 1 Device parameters of GFET

Device Parameter	Value
Thickness of gold contact (t_Au)	50nm
Thickness of SiO_2 (t_SiO_2)	6nm
Thickness of Silicon (t_Si)	300nm
Gold contact length (L_contact)	500nm
Drain voltage (V_d)	10mV
Gate voltage (V_{tg})	0 V
Source voltage (V_s)	0 V
Width (W)	4 μm
Relative permittivity (epsilonr)	4.2
Donor Concentration	$1E18cm^{-3}$

the graphene surface which can have the capability to capture the target molecule(antigen).

The working principle of the GFET biosensor can be described as follows. When a negatively charged antigen, molecule is attached to the surface, the charge carrier's depletion occurs in the complete cross-section of GFET that results in a decrease of electrical conductance and the drain current. Similarly, when a positively charged protein binds to a GFET biosensor, the conductance increases [9–12]. These properties can be demonstrated in COMSOL Multiphysics using the chemical reaction and transport of diluted spices modules, as well as the semiconductor module [13, 14]. It can be expressed quantitatively as the concentration of Antigen participating in the reaction with Antibody, as shown in Eq. (1).

$$[k]_{Ag} + [k]_{Ab} \Longleftrightarrow [k] \tag{1}$$

These antigen particles are ejected from the solution and transported to the immobilized antibodies (mAbs). This can be stated as

$$[k]_{AB} \Longleftrightarrow [k]_{Ag} \tag{2}$$

Where $[k]_{Ag}$ denotes the concentration of Antigen- SARS-CoV-2,

$[k]_{Ab}$ represents the concentration of SARS-Cov-2 mAb,

$[k]$ signifies the complex concentration,

$[k]_{AB}$ symbolizes the concentration of SARS-CoV-2 in the bulk fluid.

The modelling was done for low fluid quantities and small-scale designs. As a result, the flow is considered laminar because there is no turbulence and it is a steady flow [15].

$$\frac{\partial \rho}{\partial t} + \rho(\nabla . U) = 0 \tag{3}$$

$$\rho\left[\frac{\partial U}{\partial t} + U(\nabla . U)\right] = -\nabla P + F + \mu(\nabla . U) \tag{4}$$

Where P denotes pressure in Pascal, F denotes body force, U denotes velocity, μ -dynamic viscosity, and - ρ density.

By considering Fick's second law, diffusion of Antigens is expressed as

$$\frac{\partial C}{\partial t} = \chi \frac{\partial^2 C}{\partial x^2} \tag{5}$$

In which the term ∂C/∂t is the accumulation which is expressed in $cm^{-3}\ s^{-1}$,

χ is the diffusivity in $cm\frac{2}{s}$

The preceding equations are solved using small volume elements to discretize the sensor area. As illustrated in Fig. 2(b), the user-defined mesh is used which consisting of triangular or mapped elements with a GFET mesh refinement structure. It was stated that there would be 100 iterations. The mesh variations produced for various element numbers are

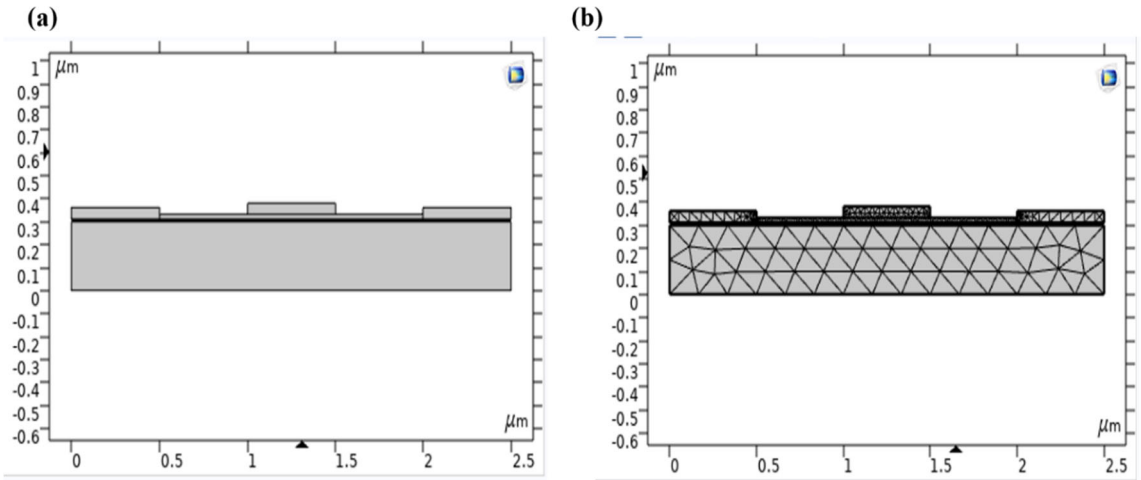

Fig. 2 Design structure of (**a**) GFET (**b**) Mesh structure of GFET

reassuringly similar. Finalized geometry consists of three domains, sixteen boundaries, sixteen vertices, and twenty-eight edges. The entire mesh comprises 6856 domain elements, 1465 boundary elements, and 386 edge elements.

3 Materials & Methods

The general characteristics of a sensing material (which are used in different field effect transistors) are very much sensitive at lower densities. Hence, micrometre-sized sensors fabricated from graphene were capable of detecting individual molecules attaching to or detaching from the surface. As the addition or removal of a molecule causes a change of one electron within the graphene structure, small step-like changes in resistance can therefore be measured. A graphene material thickness of 0.35nm is used for the detection of virus particles which is highly sensitive.

Graphene was moved to a SiO2/Si substrate utilizing ordinary wet-move strategies. Poly(methyl methacrylate) (PMMA) C4 (Vision Polymer Pvt., Ltd, Gujarat, India) was turn covered at 500 rpm for 10 s and at 3000 rpm for 30 s onto graphene on Cu foil (Sigma-Aldrich, Bangalore, India). Poly (methyl methacrylate) (PMMA) C4 (Vision Polymer Pvt., Ltd, Gujarat, India) was turn covered at 500 rpm for 10 s and 3000 rpm for 30 s onto graphene on Cu foil (Sigma-Aldrich, Bangalore, India). PMMA/graphene on Cu foil was scratched in CE-100 copper etchant (MG chemicals, India). After the Cu foil was scratched, the PMMA/graphene layers were moved to utilize clean glass slides into a deionized (DI) water (Astraa chemicals, Chennai, India), and the copper etchant was laved. Consequently, the PMMA/graphene layer was moved to a SiO2/Si substrate and dried under surrounding conditions for the time being. To make useful graphene-based devices, the graphene was patterned into required shapes by the photolithography method Fig. 3(a-c).

Arbitrary nature of shed graphene made utilizing of EBL inescapable in GFET manufacture measure. One-step and two-steps e-shaft lithography is applied for back-gate and top-gate gadgets separately. Roughly 200 nm PMMA (A2) was spinned as EBL oppose, and was uncovered by Raith Turnkey 150 SEM and E-shaft lithography framework. The rGO was ready by chemical reduction technique with hydrazine, which is considered as standard reductant for GO. Hydrazine can successfully eliminate the oxygen-containing gatherings [16] Fig. 3(d-e). Immobilization is also one of the important steps to analyze the characteristics of the designed GFET as it is to be equipped with SARS-CoV-2-Spike protein C-terminal antibody (Sigma-Aldrich, Bangalore, India) to identify the respective SARS-CoV-2 antigens (Sigma-Aldrich, Bangalore, India).

In GFET bio-sensors, dopped channels are substituted with graphene material and these gate terminals are replaced with bio-receptors. Despite the differences in structure, GFET sensors work in the same way as regular FET sensors. The conductivity of GFET is changed by charged particles that are attached to them. The oxide layer acts as an isolation layer on the Si surface of bio-sensors. Even though charged biomolecules accumulated on the oxide layer, the conductivity of the sensor will not be affected [17–20]. Pure graphene is not that sensitive to charged bioparticles. Hence, the surface of GFET must be functionalized. The functionalization may include receptors are to be attached to these sensors for the detecting of the specifically charged biomolecules (target molecules). With this, chemical connections between the surface of graphene and biomolecules can be established. The receptors along with target molecules, create an electric field on the surface of the GFET bio-sensor and which will bring a considerable change in the conductivity of the sensor.

When we consider receptors along with target particles as an input, the receptors function similar to that of the gate (as they are on the surface of graphene) in that they convert the input signal to bring changes in the conductivity of the sensor [21]. Hence, one of the most essential factors in identifying target particles (SARS-CoV-2 Antigen) is the functionalization of GFET. For this immobilization process, firstly GFET sensor was salinized with Glutaraldehyde. Further, it is treated with EDC (1-ethyl-3-(3-dimethylamino) propyl carbodiimide, hydrochloride (Sigma-Aldrich, Bangalore, India), and Sulfo-NHS (Sigma-Aldrich, Bangalore, India) to make mAb immobilized as shown in the Fig. 4.

We must equip GFET with receptor particles (SARS-CoV-2 mAb) to identify the target molecules. Figure 4 depicts the general binding process using 3-aminopropyltriethoxysilane (APTES), which acts as a receptor [22, 23]. APTES breaks down silicon-oxygen bonds to form a layer in which the specific receptor is present. Immobilization of receptor particles on the surface of the sensor starts with salinization of the sensor with Glutaraldehyde. Afterward, EDC (1-ethyl-3-(3-dimethylamino) propyl carbodiimide, Hydrochloride, and Sulfo-NHS are used for protein cross-linking and immobilization. The electrical characteristics of the designed sensor are calculated. Later on, they compared the characteristics of the sensor with the presence of SARS-CoV-2 mAb and in the non-existence of coronavirus particles (SARS-CoV-2). The conductance is relatively more when compared to the bare GFET conductance. The current is increased when mAb is attached to the GFET sensor. The results obtained were discussed in the next section.

4 Results and Discussion

4.1 Morphological Characterization

To affirm that the GFET biosensor was perfectly designed, definite characterization was performed after each progression

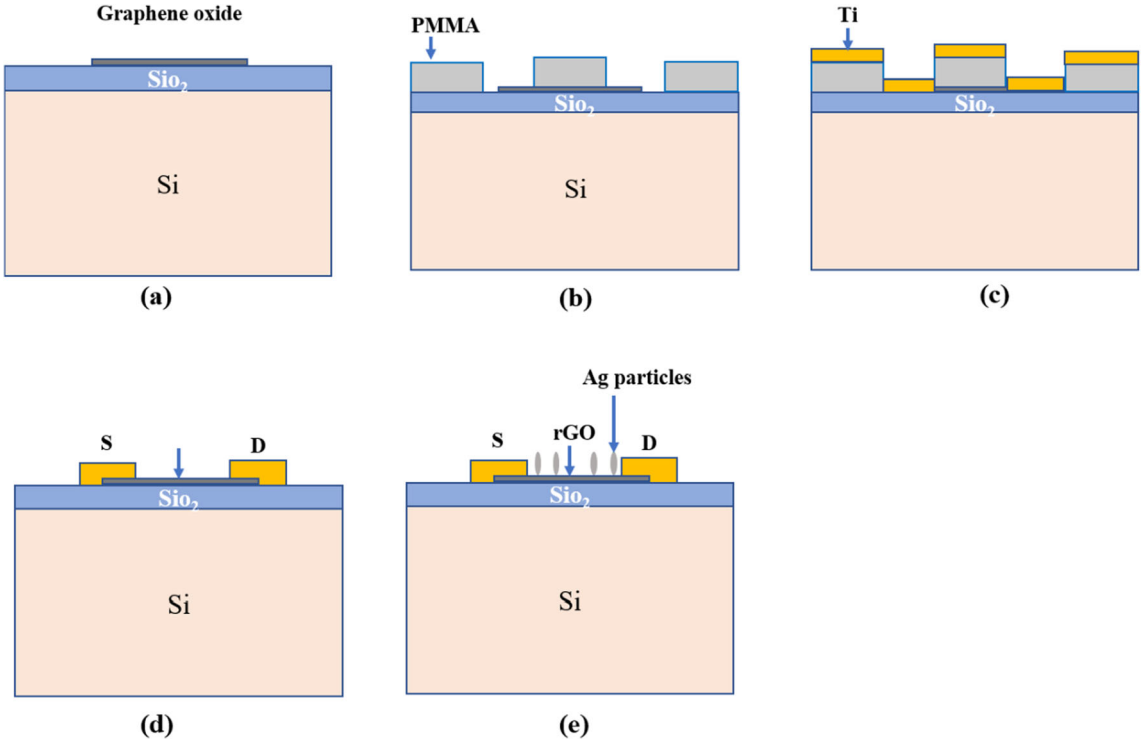

Fig. 3 Fabrication flow GFET, (**a**) Graphene oxide placed on Silicon Substrate, (**b**) PMMA coating acts as resist, (**c**) Physical Vapour Deposition of Titanium, (**d**) Lift-off of Titanium identify terminals of GFET, (**e**) rGO by chemical reduction technique with hydrazine

of functionalization. The scanning electron microscopy (SEM) used for validation, which introduced a homogeneous and high thickness of rGO surface. Image of rGO sheets as seen through a scanning electron microscope shown in Fig. 5(a). rGO sheets which are having less layers have been stacked and attempted to limit the wrinkles and foldings by utilizing transmission microscope (TEM). The TEM image of rGO sheet was shown in Fig. 5(b), which has layers of the order ($n < 6$). HRTEM micrograph of rGO sheets and it plainly shows the grid edges of graphene. This gives extra data about the interplanar distance d002 for rGO material which worth is 3.850 Å. The crystallographic design of the graphene sheets was portrayed by selected area electron diffraction (SAED) technique. The past investigations referenced that the majority of the graphene sheets showed a solitary arrangement of hexagonal diffraction design with sharp and clear diffraction spots [x] as shown Fig. 5(c). SAED pattern of reduced graphene oxide. The obtained SAED data show unambiguously that the sample RGO differs from Graphite 2 H PDF 75-1621 and has typical interplanar distance d002 from 3.586 Å up to 4.016 Å for three different RGO samples Fig. 5(d).

4.2 Electrical Characterization

To determine the electrical characteristics, the thickness of silicon is considered as 300nm the thickness of silicon dioxide is considered as 6nm. The conductance of the channel is assessed according to the available charging carriers, which are affected by the voltage of the gate. In return, the driving controls the current of the drain terminal. The drain (I_d) is measured with a constant drain voltage of 2 V, 4 V, and 6 V when the source is

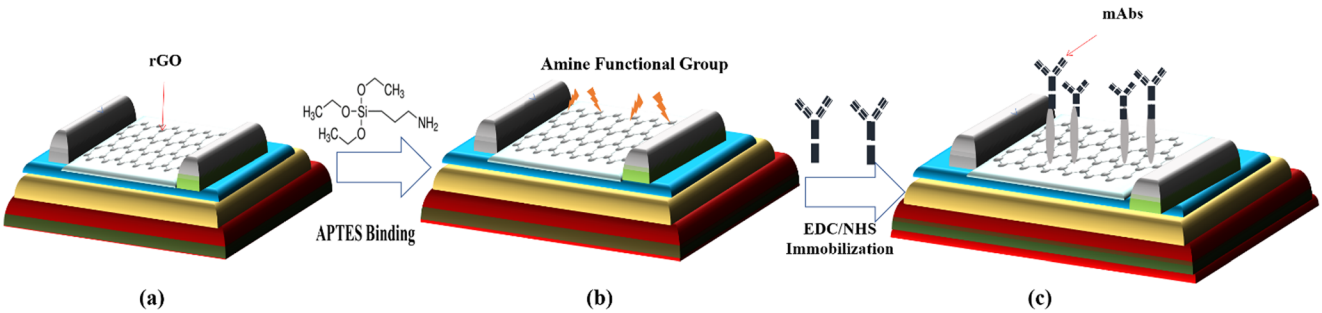

Fig. 4 Procedural steps for immobilization of SARS-CoV-2 mAb: (**a**) Reduced graphene oxide FET (**b**) GFET with amine functional group on the graphene surface through APTES binding and (**c**) Immobilization of mAbs with EDC/NHS

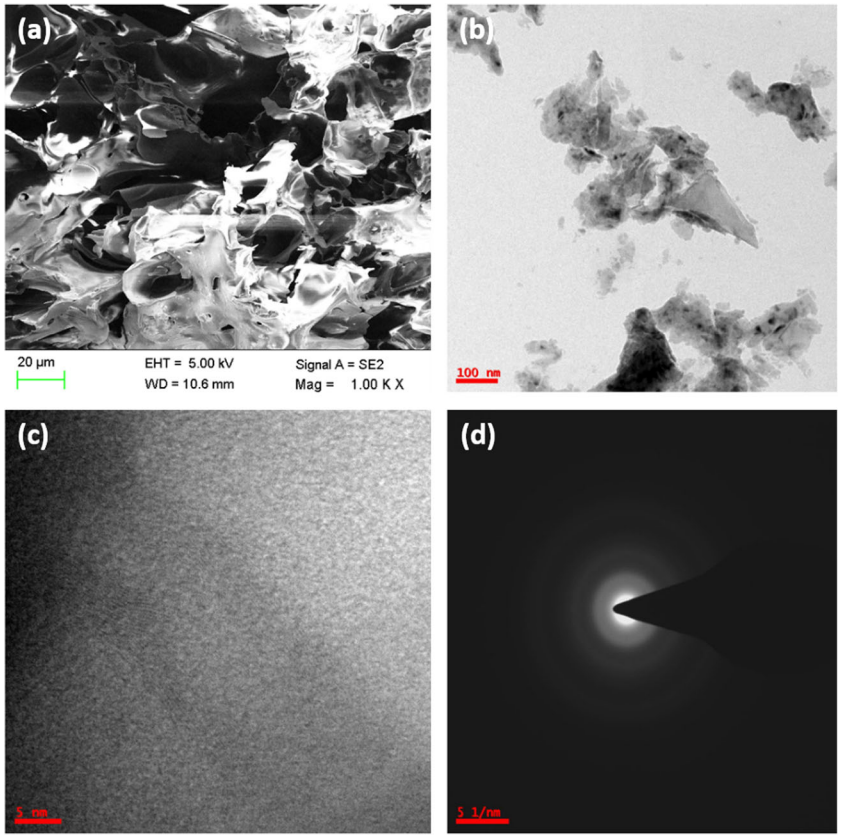

Fig. 5 Images of reduced graphene oxide nanocomposites: (**a**) SEM (**b**) TEM (**c**) HRTEM and (**d**) SAED

connected to the ground. The drain current (I_d) is calculated in the drain characteristics by sweeping the drain voltage from 0 to 20 V at various constant gate voltages (V_g) such as 6 V, 8 V, and 1 V. The results of the simulation are very similar to the results of the experimental sensor in terms of accuracy for both characteristics as shown in Fig. 6(a) and (b).

A current of the nano-ampere order comes with the characteristics of the bare GFET. With small voltage sizes, the I-V special behavior of the GFET utilizes the ability to identify charged molecules (present at the surface of the sensor) with detectable current changes. The small change in the drain current along the graphene gives an overview of the I_d-V_d curve. The biosensor was used to detect coronavirus antigens by the measurement of current in the circuit The GFET is exposed to mAbs and antigens with which analyzed the performance characteristic changes to be applied voltages. To perform this analysis, the drain voltage is varied in the range of 0 to 50 V, with the different concentrations of SARS-CoV-

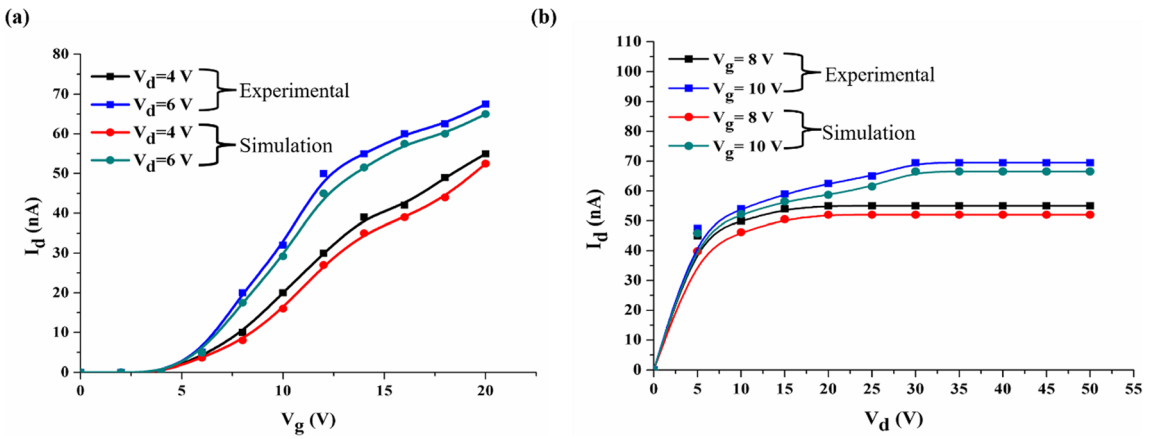

Fig. 6 Electrical characteristics of the GFET (**a**) V_g-I_d (**b**) V_d-I_d

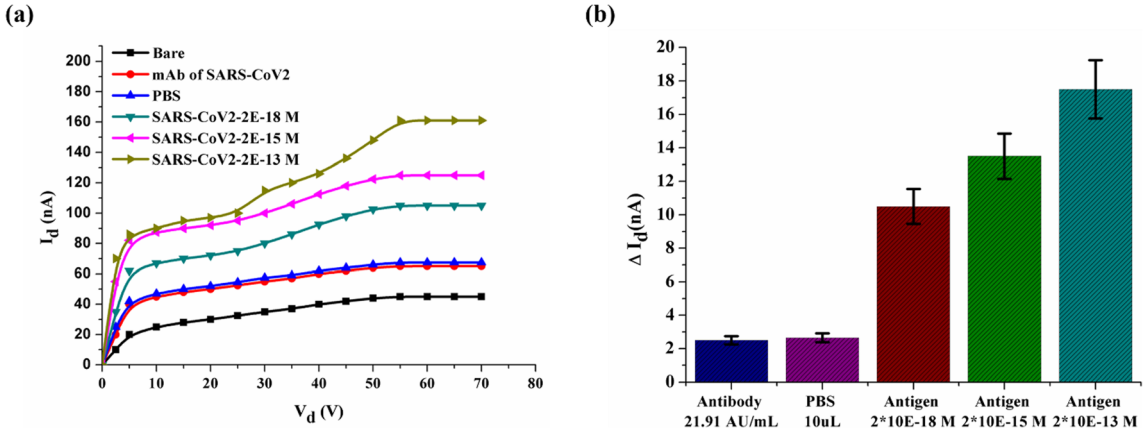

Fig. 7 Analytical characteristics of GFET (**a**) Drain current with different concentrations of antigen (**b**) change in drain current with different concentrations of antigen

2 like 2*10E-13 M, 2*10E-15 M, and 2*10E-18 M. An adsorption concentration of one molecule per square nanometer of the biomarker was considered on the surface of the gate.

In this analysis, a linear dependence of the transistor's current value on the tested quantity of antigens is observed. The Biosensor Current is modulated by antibody-antigens bindings as specific protein is on the surface. The drain characteristics are evaluated in the presence of SARS-CoV-2mAb to check the sensitivity of this GFET about the coronavirus particles, compared to a reference test in the absence of SARS-CoV-2. When SARS-CoV-2 exists concerning the design parameters, the designed GFET changes its drainage current. The maximum current without any virus particle is 70 nano-amperes, whilst the maximum drain current raises to 170 nano-amperes in the presence of antigen.

Firstly, the drain current of the designed sensor without mAbs has been calculated. The order of the 70-nano-ampere is then observed in the current as shown in Fig. 7(a). The current raised to 50 nano-amperes by load accumulated because of antibody present when it was fitted with SARS-CoV-2 MAb. Furthermore, when the sensor reacted with PBS solution, there is no current change observed. The sensor is subsequently equipped with different antigen concentrations, then the current is amplified according to SARS-Cov-2 antigens. The current is shown as 170 nA for the 2E10-18 M concentration. The change drain current (ΔI_d) with an error (± 10 %) value, with respect to different concentrations of antigen is shown in Fig. 7(b). The maximum current change is observed with antigen of concentration of 2E-13 M which the order of 18 nA which is 9 times of antibody concentration's current change with which we can conclude that antigen with higher concentration leads to higher current changes. Based on 3-fold of signal to noise ratio, the limit of detection was determined to be 0.002 fM. Additionally, Fig. 7(b) gives a more instinctive show and comparison. As we can observe, the detecting signals delivered with various concentrations of samples were stronger than those in PBS at a similar concentration of target, in comparison with the background baseline (3-fold of blank), with satisfactory detection limits, they were still significant and measurable. The comparative analysis of different FETs based platforms for the detection of various virus diseases is shown in Table 2. Among all the designed GFET shown excellent limit of detection value.

5 Conclusions

In this work, reduced Graphene FET was designed and characterized. The GFET characteristics were observed in different extents. These device characteristics are sensitive to

Table 2 Limit of detection comparison with various FET immunosensors

Virus Type	Type of Immunosensor FET	Limit of detection	Ref.
Hepatitis-B Virus	Tailored DG FET	1.5 fM	[24]
SARS-CoV N protein	Carbon nanotube FET (CNTFET)	5 nM	[25]
SARS-CoV N protein	High-Electron Mobility Transistor FET (HEMT)	0.003 nM	[26]
SARS-CoV-2	SiNW FET	1fM	[27]
SARS-CoV-2	Graphene	0.2 pM	[28]
SARS-CoV-2	Graphene	0.002fM	This Work

charged biomolecules. This study shows that the presence of the SARS-CoV-2 virus (antibody-antigen binding), greatly affects the electrical properties of the designed GFET so as the sensor characteristics. The device is sensitive to biomolecules adsorbed by the receptor. Very diluted coronavirus detections were obtained at 2E-18 M. The designed GFET is a strong device to rapidly screen virus proteins, small biomolecules, and different biomarkers. These biosensors are especially advanced for future biomedical applications, such as diagnosis of virus infection and lab-on-chip platforms also.

Acknowledgements The authors would like to acknowledge Indian Institute of Technology Hyderabad (IIT Hyderabad) for backing us with some experimental work carried out and the tool (COMSOL Semiconductor Module) required for simulating this work. And M. Durga Prakash thankfully acknowledges this publication as an outcome of the R&D work undertaken project under the Start-up Research Grant (File No.: SRG/2019/002236) scheme of Department of Science and Technology (DST), Government of India, being Science Engineering Research Broad (SERB).

Author Contributions M. Durga Prakash, B. Vamsi Krsihna and Shaik Ahmadsaidulu: Conceptualization; M. Durga Prakash, B. Vamsi Krsihna and Shaik Ahmadsaidulu: investigation; M. Durga Prakash, Shaik Ahmadsaidulu, B. Vamsi Krsihna, and B: resources; M. Durga Prakash, Shaik Ahmadsaidulu, B. Vamsi Krsihna and Surapaneni Sai Tarun Teja, D Jayanthi, Alluri Navaneetha and P Rahul Reddy: data curation; M. Durga Prakash, Surapaneni Sai Tarun Teja, D Jayanthi, Alluri Navaneetha, P Rahul Reddy and Shaik Ahmadsaidulu: writing—original draft preparation; M. Durga Prakash, B. Vamsi Krsihna, and Shaik Ahmadsaidulu: writing—review and editing; M. Durga Prakash and Shaik Ahmadsaidulu: visualization; M. Durga Prakash: supervision;

Data Availability No supplementary materials.

Declarations

Conflict of Interest The authors declare that they have no conflict of interest.

Human and Animal Rights This article does not contain any studies with human or animal subjects.

Consent to Participate Additional informed consent was obtained from M. Durga Prakash identifying information is included in this article.

References

1. Wu F, Zhao S, Yu B, Chen YM, Wang W, Song ZG, Hu Y, Tao ZW, Tian JH, Pei YY, Yuan ML (2020) A new coronavirus associated with human respiratory disease in China. Nature 579:265–269. https://doi.org/10.1038/s41586-020-2008-3
2. WHO. Novel Coronavirus (2019-nCoV) Situation Report – 1. https://www.who.int/docs/default-source/coronaviruse/situationreports/20200121-sitrep-1-2019-ncov.pdf?sfvrsn=20a99c10_4 (2020-04-15)
3. Coronavirus Disease (COVID-19) Pandemic. Available online: https://www.who.int/ru/emergencies/diseases/novel-coronavirus-2019. Accessed 1 July 2021
4. Jayaweera M, Perera H, Gunawardana B, Manatunge J (2020) Transmission of COVID-19 virus by droplets and aerosols: A critical review on the unresolved dichotomy. Environ Res 188:109819. https://doi.org/10.1016/j.envres.2020.109819
5. Echtioui A, ZouchW, Ghorbel M, Mhiri C, Hamam H. Detection methods of COVID-19. SLAS Technol 25(6):566–572. https://doi.org/10.1177/2472630320962002
6. FroylaÂn Ibarra N, Montenegro Y, Vera C, Boulard H, Quiroz J, Flores P, Ochoa (1998) Comparison of three ELISA tests for seroepidemiology of bovine fascioliosis. Vet Parasitol 77:229–236. https://doi.org/10.1016/S0304-4017(98)00111-3
7. BV, Krsihna S, Ravi, Prakash MD. Recent developments in graphene based field effect transistors. Mater Today Proc. https://doi.org/10.1016/j.matpr.2020.07.678
8. Ahmadsaidulu S, Durga Prakash M (2021) Impacts of gate length and doping concentrations on the performance of silicon nanowire Field effect Transistor. Mater Today Proc 46(Part 9):3693–3698. https://doi.org/10.1016/j.matpr.2021.01.849
9. Matta DP, Vanjari SRamaK, Sharma CS, Singh SG (2016) Ultrasensitive, label free, chemiresistive nanobiosensor using multiwalled carbon nanotubes embedded electrospun SU-8 nanofibers. Sensors 16(9):1354. https://doi.org/10.3390/s16091354
10. Prakash MD, Tripathy S, Vanjari SRamaK, Sharma CS, Singh SG (2016) An ultrasensitive label free nanobiosensor platform for the detection of cardiac biomarkers. Biomed Microdevices 18(6):1–10. https://doi.org/10.1007/s10544-016-0126-3
11. Fan Yang G-J, Zhang (2014) Silicon nanowire-transistor biosensor for study of molecule-molecule interactions. Rev Anal Chem 33(2):95–110. https://doi.org/10.1515/revac-2014-0010
12. Fernando Patolsky, Brian P, Timko G, Zheng, Lieber CM (2007) Nanowire-based nanoelectronic devices in the life sciences. MRS Bull 32(2):142–149. https://doi.org/10.1557/mrs2007.47
13. Tabatabaian M (2015) CFD module. Stylus Publishing, LLC, Sterling
14. Multiphysics C (2015) Chemical reaction engineering module user's guide. COMSOL AB, Stockholm
15. Hajji L, Kolsi W, Hassen AAAA, Al-Rashed MN, Borjini MA, Aichouni (2018) Finite element simulation of antigen-antibody transport and adsorption in a microfluidic chip. Phys E 104:177–186. https://doi.org/10.1016/j.physe.2018.07.034
16. Adriano Ambrosi CK, Chua A, Bonanni, Pumera M (2012) Lithium aluminum hydride as reducing agent for chemically reduced graphene oxides. Chem Mater 24:2292–2298. https://doi.org/10.1021/cm300382b
17. Puurunen RL (2005) Surface chemistry of atomic layer deposition: A case study for the trimethylaluminum/water process. J Appl Phys 97:121301. https://doi.org/10.1063/1.1940727
18. Shen M-Y, Li B-R, Li Y-K (2014) Silicon nanowire field-effect-transistor based biosensors: From sensitive to ultra-sensitive. Biosensors Bioelectronics 60:101–111
19. Lieber CM. Nanoscale science and technology: building a big future from small things. MRS Bull 28(07):486–491. https://doi.org/10.1557/mrs2003.144
20. Yue Wu J, Xiang C, Yang W, Lu, Charles M, Lieber. Single-crystal metallic nanowires and metal/semiconductor nanowire heterostructures. Nature 430(6995):61–65
21. Zheng G, Lu W, Jin S, Lieber CM (2004) Synthesis and fabrication of high-performance n-type silicon nanowire transistors. Adv Mater 16(21):1890–1893
22. Cui Y, Wei Q, Park H, Lieber CM (2001) Nanowire nanosensors for highly sensitive and selective detection of biological and chemical species.. Science 293(5533):1289–1292
23. Chunyu, Chan et al (2017) A microfluidic flow-through chip integrated with reduced graphene oxide transistor for influenza virus gene detection. Sens Actuators B 251(1November):927–933. https://doi.org/10.1016/j.snb.2017.05.147

24. Lee I-K, Jeun M, Jang H-J, Cho W-J, Lee KH (2015) A self-amplified transistor immunosensor under dual gate operation: highly sensitive detection of hepatitis B surface antigen. Nanoscale 7: 16789–16797. https://doi.org/10.1039/C5NR03146J
25. Ishikawa FN, Curreli M, Olson CA, Liao HI, Sun R, Roberts RW, Cote RJ, Thompson ME, Zhou C (2010) Importance of controlling nanotube density for highly sensitive and reliable biosensors functional in physiological conditions. ACS Nano 4:6914–6922. https://doi.org/10.1021/nn101198u
26. Hsu Y-R, Lee G-Y, Chyi J-I, Chang C-k, Huang C-C, Hsu C-P, Huang T-h, Ren F, Wang Y-L (2013) Detection of Severe Acute Respiratory Syndrome (SARS) coronavirus nucleocapsid 682 protein using AlGaN/GaN high electron mobility transistors. ECS Trans 50:681. https://doi.org/10.1149/05006.0239ecst
27. Chua JH, Chee R-E, Agarwal A, Wong SM, Zhang G-J (2009) Label-free electrical detection of cardiac biomarker with complementary metal-oxide semiconductor-compatible silicon nanowire sensor arrays. Anal Chem 81(15):6266–6271. https://doi.org/10.1021/ac901157x
28. Xiaoyan, Zhang et al (2020) Electrical probing of COVID-19 spike protein receptor binding domain via a graphene field-effect transistor. ArXiv:2003.12529 [Cond-Mat, Physics: Physics]. http://arxiv.org/abs/2003.12529